# Broadband low-repetition-rate mode-locked fiber laser for swept source optical coherence tomography

Laiyang Dang[a,b], Wenhao Zhu[a,b], Dongmei Huang[a,b,*], and Feng Li[b]
[a]Photonics Research Institute, Department of Electrical and Electronic Engineering, The Hong Kong Polytechnic University, Hong Kong SAR, China;
[b]The Hong Kong Polytechnic University Shenzhen Research Institute, Shenzhen 518057, China;
*Corresponding author: meihk.huang@polyu.edu.hk

## ABSTRACT

We proposed and demonstrated an all-fiber nonlinear polarization rotation (NPR) erbium-doped mode-locked laser, which reduces the laser repetition rate to 5.7 MHz based on a large mode area fiber (LAMF). In addition, the laser 3 dB bandwidth is extended to 86.4 nm by using extra cavity supercontinuum broadening. To the best of our knowledge, this is the first time to obtain a broadband output using such a low repetition rate mode-locked laser. This broadband low repetition rate mode-locked laser signal is then applied to time-stretched optical coherence tomography (OCT). The swept source can achieve an imaging range of more than 85 mm and a sensitivity roll-off of 3.5 dB in OCT. The all-fiber low repetition rate broadband swept source based on time-stretching technology has a compact structure and high stability, and is very promising in the field of frequency measurement and high-resolution OCT.

**Keywords:** Broadband low-repetition-rate, mode-locked fiber laser, optical coherence tomography, swept source, spectral broadening

## 1. INTRODUCTION

Optical coherence tomography (OCT) with non-destructive characteristics, high resolution and real time imaging has been widely applied in medical analysis, biological imaging and industrial detection[1-3]. Compared with time domain OCT and spectral domain OCT, swept source OCT has high speed since it utilizes a high photodiode to acquire the interference signal in the time domain, which is the next generation of OCT[4,5]. The key of swept source OCT (SS-OCT) system is the swept source, whose sweep rate, sweep range and coherence length determine the imaging speed, resolution and imaging range, respectively[6]. Different techniques including short cavity swept laser with a tunable filter, vertical-cavity surface-emitting lasers (VCSELs) and Fourier-domain mode-locked fiber laser have been proposed to realize swept lasers[7-9]. However, the sweep rate is limited due to the mechanical tuning elements and the coherence length is only several millimeters or tens of millimeters. Time stretching a broadband and highly coherent ultrashort mode locked pulses can obtain a high sweep rate and high coherence swept laser[10-14]. Due to the detection bandwidth of the photodiode, MHz sweep rate swept laser is a good candidate to realize high imaging speed as well as long imaging range. Therefore, a mode locked laser with long cavity to realize MHz repetition rate is desirable. However, it is difficult to achieve stable single pulse laser operation due to the accumulation of nonlinear phase shift resulting in pulse splitting caused by longer fibers. In addition, the limitation of the gain bandwidth and the serious mismatch of the dispersion in the resonator makes it a great challenge to obtain highly coherent pulses with a sufficiently wide spectrum.

In this work, we proposed and experimentally demonstrated a low repetition rate mode-locked fiber laser based on a large mode area fiber (LMAF). The low nonlinearity of LMAF is used to reduce the laser repetition rate and achieve single pulse self-starting operation of the laser. In addition, the dispersion compensation fiber (DCF) is inserted at different positions in the laser to make the intracavity dispersion appear in a breathing state to compensate the intracavity dispersion and further reduce the nonlinear effect. Subsequently, the mode-locked laser pulse is amplified and compressed, and then injected into a high nonlinear optical fiber (HNLF) for extra-cavity spectral broadening. Eventually, a high-coherence single-pulse laser with a 3 dB bandwidth of ~86.41 nm and a repetition rate of 5.7 MHz is obtained. The pulses are time-stretched by DCF that equivalently compensated 80 km of G.652 single-mode fiber (SMF) to form a reconfigurable wide-spectrum high-speed swept source. This broadband and highly coherent swept laser with

Fifteenth International Conference on Information Optics and Photonics
(CIOP 2024), edited by Yue Yang, Proc. of SPIE Vol. 13418, 134183F

5.7 MHz sweep rate is finally applied in the swept source OCT system, where a 3.5 dB sensitivity roll-off length of 170 mm and an axial resolution of approximately ~35 μm are achieved. The proposed swept source has unique advantages in improving the imaging performance of SS-OCT, LiDAR and optical frequency domain reflectometry (OFDR).

## 2. EXPERIMENTAL SETUP

The experimental setup is shown in Fig. 1, where the erbium-doped fiber (EDF) act as a gain medium of the mode-locked fiber laser. To reduce the repetition rate of the laser, a 30 m large mode area fiber (LAMF) with a low nonlinear coefficient is used to increase the cavity length. Two sections of 2 m dispersion compensation fiber compensate the intracavity dispersion to near-zero dispersion to obtain a relatively flat and broadband spectrum. In addition, the splicing loss introduced by DCF will further reduce the nonlinear effect in LAMF. The use of a tap-isolator wavelength division multiplexer (TI-WDM) makes the laser system more concise to reduce the length of the single-mode fiber (SMF). A polarization controller (PC) is used to optimize the polarization state of light to control the polarization and nonlinearity in the laser cavity to achieve laser mode locking. Note that 20% of the light is reflected by the TIWDM for the next supercontinuous broadening purpose. The function of the isolator (ISO) is to prevent the influence of the reflected light of the all-normal-dispersion (ANDi) supercontinuum broadening system on the laser mode-locked state. Here, a 9 m SMF-28e with a dispersion of 17 ps/nm/km at 1550 nm is used to compress the pulse width to increase the single pulse energy. A 978nm pump 2, a WDM and a 2 m erbium doped photosensitive fiber (ESF) with a dispersion of 16 ps/nm/km constitute the laser amplification system. A 5 m ANDi highly nonlinear fiber (ANDi-HNF) with a dispersion of -5 ps/nm/km is used to achieve spectral broadening of the mode-locked laser. The broadband spectrum pulse laser is injected into a 10 km DCF for time stretching to obtain a swept laser signal. Finally, a swept source OCT system is formed by using a Michelson interferometer with a scanning galvo mirror to achieve high-resolution imaging of objects.

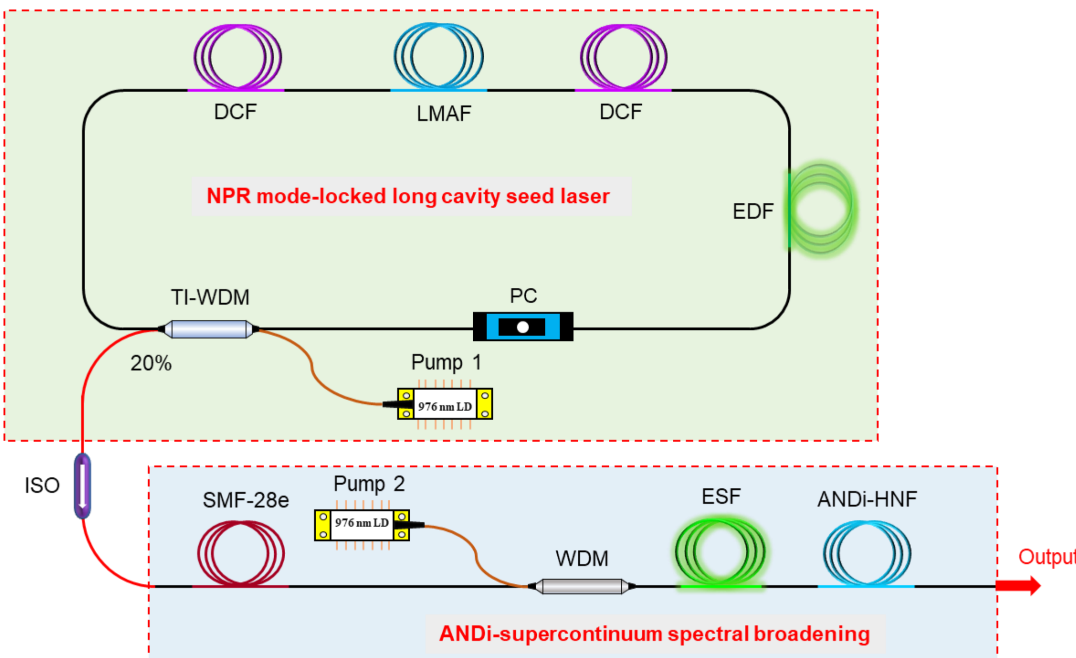


Figure 1. Experimental setup of the broadband low-repetition-rate mode-locked fiber laser.

## 3. EXPERIMENTAL RESULTS AND DISCUSSION

The NPR mode locking is achieved by setting the pump power to 50 mW and precisely adjusting the polarization state to control the intracavity nonlinearity. Figure 2(a) shows the spectrum of the broadband mode-locked laser measured by an optical spectrum analyzer (OSA), with a 3 dB bandwidth of 6.1 nm. An electrical spectrum analyzer (ESA) with a resolution bandwidth of 10 kHz is used to measure the radio frequency (RF) spectrum. Figure 2(b) shows that at a fundamental repetition rate of 5.7 MHz, the signal-to-noise ratio (SNR) of the pulse train can be as high as ~ 92.4 dB, indicating that the seed laser operates in a stable mode-locked state. The seed laser is injected into the supercontinuum broadening system to achieve spectrum broadening. The e amplified spontaneous emission (ASE) spectrum of ESF and the broadened spectrum under different pump powers are shown in Fig. 2(c). It can be seen that the spectrum will be continuously broadened with the increase of pump power, but the influence of ASE will also be aggravated. The measured supercontinuum broadening spectrum reaches the optimum when the power of pump 2 reaches 620 mW, and its 3db bandwidth and 10 dB bandwidth are 86.41nm and 113.535nm, respectively, as shown in Fig. 2(d). To further study the supercontinuum spectrum broadening characteristics, different spectral bandwidths during the pump power increase of the amplifying system are calculated are shown in Fig. 2(e). Here, the 10 dB bandwidth evolution result shows that the spectrum will continue to broaden with the increase of pump power, while the 3 dB bandwidth shows that the spectrum becomes uneven. Therefore, the pump power needs to be adjusted appropriately to achieve a flat broadband spectrum output.

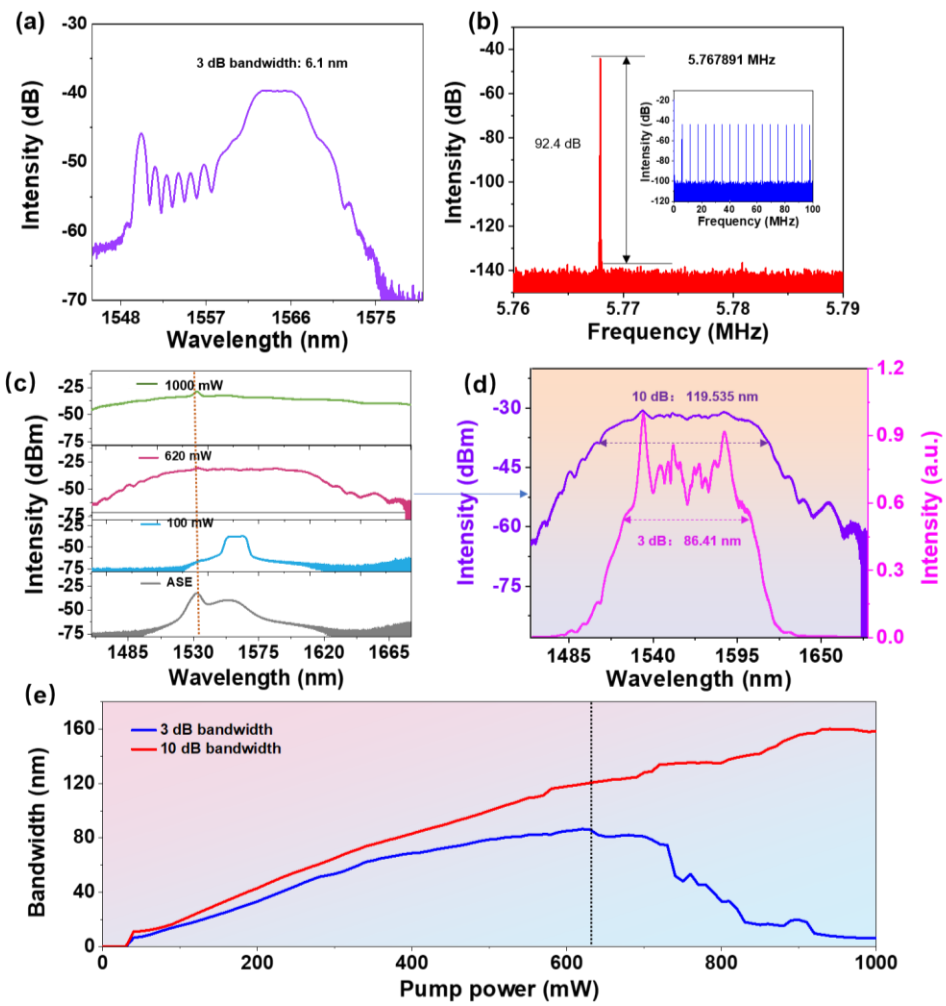


Figure 2. (a) The direct output optical spectrum of the long cavity seed laser. (b) The RF spectrum of the mode-locked seed laser. (c) ASE spectrum of ESF and supercontinuous broadening spectra at different pump power. (d) The spectrum in linear (purple curve) and logarithmic (blue curve) at a pump power of 620 mW. (e) 3 dB and 10 dB bandwidths of supercontinuum spectra versus pump power.

Figure 3(a) shows the modulated interference fringes captured by a high-speed oscilloscope. The modulation of the interference signal is caused by the optical path difference between the two arms of the Michelson interferometer, which helps to accurately obtain the depth information of the sample. The resampled interference signal in the frequency domain is obtained through the swept trace, and then used for fast Fourier transform (FFT) with zero padding to calculate its point spread function (PSF), as shown in Figure 3(b). The axial resolution is measured to be 35 μm by Gaussian fitting of one of the PSF peaks. A 5.7 MHz swept signal with an average power of ~5 mW is injected into the SS-OCT system, and its sensitivity roll-off length is characterized by the PSF with different path differences, as shown in Fig. 3(c). From the average power and the sweep rate 5.7 MHz, the maximum sensitivity is ∼78 dB. As a result, the interference path difference can reach up to 170 mm when the sensitivity roll-off is 3.5 dB, which verifies that the built swept source can have the ability of deep-depth OCT imaging. In addition, the optical delay can be further increased to verify the roll-off path difference of 6 dB and 10 dB. Next, the three overlapping rough and transparent plastic plates will be imaged using the high-resolution and deep-depth SS-OCT system. As shown in Fig. 3(d), three layers of plastic plates can be clearly identified, corresponding to four reflective surfaces with a thickness of 0.5 mm. The different reflectivity of the plastic plates are also clearly identified at different demodulation intensities. In addition, the microstructure of the air layer formed by a layer of tape between the first and second plastic plates and the rough structure of the surface are also clearly visible. The SS-OCT imaging system with such high resolution will have important applications in biomedical fine imaging and other industrial precision detection.

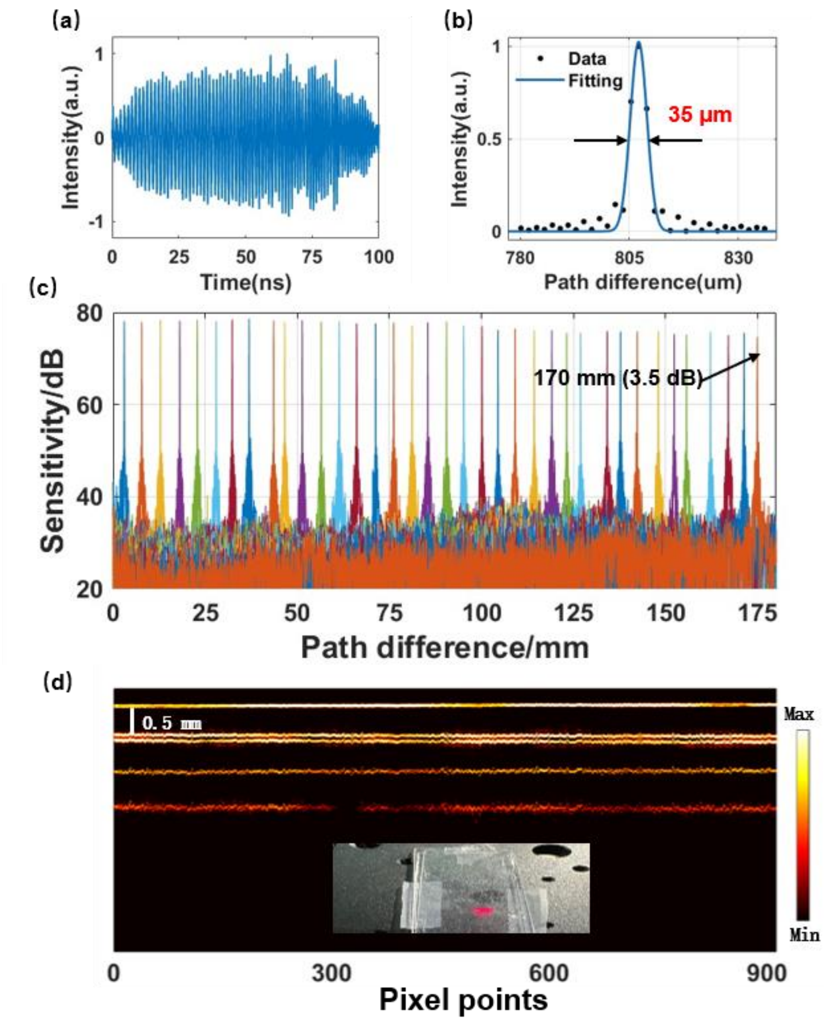


Figure 3. (a) Real-time single-shot interferogram generated by the SS-OCT system. (b). A single A-scan showing an axial resolution of 35 μm in air. (c) Roll-off of PSFs measured by the SS-OCT system under various optical path differences. (d) OCT image of three overlapping roughened and transparent plastic plates.

## 4. CONCLUSION

In this work, we propose an all-fiber long-cavity NPR mode-locked laser with a repetition rate of 5.7 MHz and a SNR of 92.4dB based on LAMF, and verify it by carefully controlling the dispersion and nonlinearity in the cavity. The output spectrum 3 dB bandwidth is broadened from 6.1 nm to 86.41 nm using extra-cavity supercontinuum spectrum broadening technology. Then, the broadband low-repetition-rate mode-locked laser signal is used as a seed source to achieve swept laser output through time stretching technology, and is applied to image objects in the SS-OCT system. Finally, three overlapping rough plastic plates with microstructures were imaged at an axial resolution of 35μm. The highly stable, flat, broadband time-stretched swept source based on low-repetition-rate mode-locked laser and extra-cavity supercontinuum broadening has excellent performance in SS-OCT systems and has broad application prospects in real-time microscopic imaging and deep-depth three-dimensional lidar.

## ACKNOWLEDGMENTS

This work was supported in part by the Research Grants Council, University Grants Committee of Hong Kong SAR (PolyU15206023); in part by the Science, Technology and Innovation Commission of Shenzhen Municipality under Grant (JCYJ20210324133406018).

## REFERENCES

1. Wieser, W., Biedermann, B. R., Klein, T., Eigenwillig, C. M. and Huber, R., "Multi-megahertz OCT: High quality 3D imaging at 20 million A-scans and 45 GVoxels per second," Opt. Exp. **18**(14), 14685–14704 (2010).
2. Klein, T., Wieser, W., Reznicek, L., Neubauer, A., Kampik, A. and Huber, R., "Multi-MHz retinal OCT," Biomed. Opt. Exp. **4**(10), 1890–1908 (2013).
3. Klein, T. and Huber, R., "High-speed OCT light sources and systems [Invited]," Biomed. Opt. Express **8**(2), 828–859 (2017).
4. Wieser, W., Draxinger, W., T. Klein, Karpf, S., Pfeiffer, T. and Huber, R., "High definition live 3D-OCT in vivo: design and evaluation of a 4D OCT engine with 1 GVoxel/s," Biomed. Opt. Express 5, 2963–2977 (2014).
5. Xu, J., Wei, X., Yu, L., Zhang, C., Xu, J., Wong, K. K. Y. and Tsia, K. K., "High-performance multi-megahertz optical coherence tomography based on amplified optical time-stretch," Biomed. Opt. Express **6**(4), 1340–1350 (2015).
6. Huang, D., Li, F., Shang, C., Cheng, Z. and Wai, P. K. A., "Reconfigurable time-stretched swept laser source with up to 100 MHz sweep rate, 100 nm bandwidth, and 100 mm OCT imaging range," Photonics Res. **8**(8), 1360-1367 (2020).
7. Dhalla, A.-H., Nankivil, D. and Izatt, J. A., "Complex conjugate resolved heterodyne swept source optical coherence tomography using coherence revival," Biomed. Opt. Express **3**(3), 633–649 (2012).
8. Cook, K. T., Qiao, P., Qi, J., Coldren, L. A. and Chang-Hasnain, C. J., "Resonant-antiresonant coupled cavity VCSELs," Opt. Express **27**(3), 1798–1807 (2019)
9. Huber, R., Wojtkowski, M. and Fujimoto, J. G., "Fourier domain mode locking (FDML): a new laser operating regime and applications for optical coherence tomography," Opt. Express **14**(8), 3225–3237 (2006).
10. Li, B., Wei, X., Tan, S., Kang, J. and Wong, K. K. Y., "Compact and stable temporally magnified tomography using a phase-locked broadband source," Opt. Lett. **41**(7), 1562–1565 (2016).
11. Li, B., Zhang, C., Kang, J., Wei, X., Tan, S. and Wong, K. K. Y., "109 MHz optical tomography using temporal magnification," Opt. Lett. 40(13), 2965–2968 (2015).
12. Wei, X., Lau, A. K. S., Xu, Y., Tsia, K. K. and Wong, K. K. Y., "28 MHz swept source at 1.0 μm for ultrafast quantitative phase imaging," Biomed. Opt. Express **6**(10), 3855–3864 (2015).
13. Tan, S., Yang, L., Wei, X., Li, C., Chen, N., Tsia, K. K. and Wong, K. K. Y., "High-speed wavelength-swept source at 2.0 μm and its application in imaging through a scattering medium," Opt. Lett. **42**(8), 1540–1543 (2017).
14. Grelet, S., Jiménez, A. M., Engelsholm, R. D., Montague, P. B. and Podoleanu, A., "40 MHz Swept-Source Optical Coherence Tomography at 1060 nm Using a Time-Stretch and Supercontinuum Spectral Broadening Dynamics," IEEE Photonics J. **14**(6), 1-6 (2022).